
Article:
Kumar, P. orcid.org/0000-0002-9965-8691, Jimenez Franco, A. orcid.org/0000-0003-1292-7850 and Zhao, X. orcid.org/0000-0002-4620-2893 (2023) 3D culture of fibroblasts and neuronal cells on microfabricated free-floating carriers. Colloids and Surfaces B: Biointerfaces, 227. 113350. ISSN 0927-7765

https://doi.org/10.1016/j.colsurfb.2023.113350

Colloids and Surfaces B: Biointerfaces 227 (2023) 113350

Contents lists available at ScienceDirect

Colloids and Surfaces B: Biointerfaces

journal homepage: www.elsevier.com/locate/colsurfb

3D culture of fibroblasts and neuronal cells on microfabricated free-floating carriers

Piyush Kumar [a,b], Ana Jimenez Franco [a], Xiubo Zhao [a,c,*]

[a] Department of Chemical and Biological Engineering, University of Sheffield, Sheffield S1 3JD, UK
[b] Centre for NanoHealth, Medical School, Swansea University, Swansea SA2 8PP, UK
[c] School of Pharmacy, Changzhou University, Changzhou 213164, China

ARTICLE INFO

Keywords:
3D cell culture
Bioprinting
Biofabrication
Cell carriers
CAD
PLGA
Silk fibroin

ABSTRACT

3D cell culture is a relatively recent trend in biomedical research for artificially mimicking *in vivo* environment and providing three dimensions for the cells to grow *in vitro*, particularly with regard to surface-adherent mammalian cells. Different cells and research objectives require different culture conditions which has led to an increase in the diversity of 3D cell culture models. In this study, we show two independent on-carrier 3D cell culture models aimed at two different potential applications. Firstly, micron-scale porous spherical structures fabricated from poly (lactic-co-glycolic acid) or PLGA are used as 3D cell carriers so that the cells do not lose their physiologically relevant spherical shape. Secondly, millimetre-scale silk fibroin structures fabricated by 3D inkjet bioprinting are used as 3D cell carriers to demonstrate cell growth patterning in 3D for use in applications which require directed cell growth. The L929 fibroblasts demonstrated excellent adherence, cell-division and proliferation on the PLGA carriers, while the PC12 neuronal cells showed excellent adherence, proliferation and spread on the fibroin carriers without any evidence of cytotoxicity from the carriers. The present study thus proposes two models for 3D cell culture and demonstrates, firstly, that easily fabricable porous PLGA structures can act as excellent cell carriers for aiding cells easily retain their physiologically relevant 3D spherical shape *in vitro*, and secondly, that 3D inkjet printed silk fibroin structures can act as geometrically-shaped carriers for 3D cell patterning or directed cell growth *in vitro*. While the 'fibroblasts on PLGA carriers' model will help achieve more accurate results than the conventional 2D culture in cell research, such as drug discovery, and cell proliferation for adoptive cell transfer, such as stem cell therapy, the 'neuronal cells on silk fibroin carriers' model will help in research requiring patterned cell growth, such as treatment of neuropathies.

1. Introduction

Cell culture is the growth of cells *in vitro* under controlled laboratory conditions [1]. Conventionally, cell culture is carried out in two ways, as cell suspensions and on the flat surface of agar plates or culture flasks [1–3]. Cell suspensions are suitable for culturing prokaryotes, such as, bacteria and algae, and non-adherent eukaryotic cells. Similarly, agar plates fed with nutrients are mostly suitable for cultivating prokaryotes and several types of eukaryotic cells. For culturing the cells and tissues of higher organisms, such as mammals, cell-culture flasks are used because most mammalian cells are adherent cells which require a substrate for attachment growth and replication [1–3].

A culture flask only provides a flat two-dimensional (2D) substratum for cell adherence and does not emulate the *in vivo* environment [4]. The complex bodies of higher organisms have nearly all of their cells residing in a three-dimensional (3D) and physiologically active environment where the cells interact with each other and with the extra-cellular matrices (ECM) through a variety of cell signalling molecules and other chemical and mechanical cues [5]. Most cells, when detached from their native tissue systems and grown onto 2D plastic surfaces, become flat, divide and proliferate irregularly, and lose their natural phenotypic and physiological characteristics [6–9]. Gene expression and mRNA splicing patterns can vary considerably between 2D and 3D cultures of the same cells [10–12]. Similarly, different cell membrane proteins are biosynthesised at different rates on different substrates [13]. Moreover, primary mammalian cells are extremely sensitive to any biochemical, anatomical and topological changes in their micro-environment with the detrimental effects of 2D *in vitro* culture visible during differentiation

* Corresponding author at: School of Pharmacy, Changzhou University, Changzhou 213164, China.
E-mail address: xiubo.zhao@cczu.edu.cn (X. Zhao).

https://doi.org/10.1016/j.colsurfb.2023.113350
Received 16 October 2022; Received in revised form 7 February 2023; Accepted 12 May 2023
Available online 15 May 2023

[14,15]. Another vital attribute is cell polarity, which is easier to be maintained in a 3D culture where cells are relatively relaxed, not bound by gravity, and free to move, migrate and explore their microenvironment. For such cells as epithelial glandular cells and neuronal cells, maintenance of cell polarization is essential for directional secretion of biologically active molecules [16]. In 2D culture, the cell-to-cell interaction is also restricted to communication with adjacent cells in single plane only, whereas in 3D culture, the cells can interact with adjacent cells from any plane [17]. It is thus evident that the physiological irrelevance and other limitations of conventional 2D or monolayer cell culture methods hold a high probability of yielding inaccurate results in crucial research areas, such as drug discovery, cell-based assays, regenerative medicine, cancer and tumour modelling, organoid bio-banks, and cosmetics industries. This in turn leads to over-reliance on animal trials, which themselves are highly variable in accuracy, and may even lead to unexpected or adverse results during human trials [18]. 3D cell culture systems, therefore, hold a significant advantage by providing an *in vitro* platform for cells to maintain their native three-dimensional shapes, polarities and freedom of movement [19,20].

Structural design-wise, 3D cell culture systems are either scaffold/carrier-free or scaffold/carrier-based [21–26]. Among the scaffold-based systems are the in-scaffold systems where cells can grow throughout the inner volume of soft and diffusive scaffolds, *e.g.*, hydrogels, and the on-scaffold systems where cells can grow only on the outside of rigid scaffolds, *e.g.*, silk fibroin. While in-scaffold or in-carrier culture is good for tissue engineering and organoid culture, the on-scaffold or on-carrier culture is excellent for drug discovery, extracting cellular products such as secretory proteins, cultivating cells at a fast pace, and cell guidance and patterning [4,21,27].

A relatively rarer but potentially important area of application of 3D *in vitro* cell culture and cultivation is in *ex vivo* gene therapy in which the pluripotent stem cells are removed from a terminally ill patient's bone marrow, their genetic defects are corrected through gene editing, and the modified cells are then transplanted back into the marrow [28–31]. Blood and immune cell disorders, such as X-linked SCID, Wiskott Aldrich syndrome, sickle cell anaemia and β-thalassemia, are usually treated through such a method of gene editing and transplantation [32]. Here, the genetically corrected bone-marrow-derived cells need to be proliferated rapidly *in vitro* for their transplantation while also ascertaining that the cells do not over- or under- express any genes during the proliferation process [33,34]. But, as stated earlier, the conventional 2D culture holds a potential risk of the cells losing their potency and normal phenotypic expression. Therefore, the first 3D cell culture model described in this paper is a preliminary insight into the possibility of using 3D cell culture as a platform for rapid cell proliferation while maintaining the spherical cell shape. For this objective, mouse L929 fibroblasts were cultured on porous spherical carriers fabricated from poly (D, L-lactide-co-glycolide) or poly (lactic-co-glycolic acid) or PLGA.

Guided cell growth or *in vitro* patterned growth and differentiation of cells is another area in which 3D culture platforms are desired [27,35,36]. The diversity in culture platform's shape and size can be brought about by various sophisticated equipment including 3D bioprinters. Patterned culture of neuronal cells on biocompatible 3D carriers has the potential for cultivation and differentiation of brain tissue or ganglia for investigating neuronal diseases, neurotrophic drug discovery and for adoptive cell transfer or nerve tissue grafts for the repair and treatment of peripheral nerve damage from injuries or degeneration [37–39]. Therefore, the second 3D cell culture model described in this paper is a preliminary insight into the possibility of using 3D cell culture for developing patterned neuronal cell grafts. For this objective, rat neuronal PC12 cells were cultured on the millimetre-sized 3D structures fabricated from silk fibroin.

2. Experimental methods

2.1. Materials

Bombyx mori silkworm cocoons were obtained from Biological Science Research Centre, Southwest University, China. The L929 immortalized mouse fibroblasts and the PC12 neuron-like rat tumour cells were obtained from American Type Culture Collection (ATCC). Ultrapure high quality deionized water (DI water), filtered with a 0.2 μm filter, was used in all experiments wherever required. Unless otherwise stated, all the chemicals were commercially obtained and were of analytical grade.

2.2. Fabrication of PLGA and fibroin carriers

Porous spherical PLGA carriers (henceforth called PLGA carriers) were prepared using oil-in-water emulsion solvent evaporation technique. For this, 200 mg of amorphous PLGA powder (lactide-to-glycolide ratio = 75:25; MW = 4000–15,000) was dissolved in 8 mL chloroform to produce the organic phase. 2.5 mL of 10% ammonium bicarbonate (NH_4HCO_3) was added to the PLGA-chloroform solution. Ammonium bicarbonate acted as a porogen by dissociating and releasing minute CO_2 bubbles to yield pores in the spherical carriers. Porous PLGA carriers have shown to be better for 3D culture of cells than the non-porous or smooth ones [40]. The solution was mixed well using a homogenizer at 1200 rpm for 1 min. For the inorganic phase, 250 mL of 1% poly-vinyl alcohol (PVA) solution was prepared in a beaker. A magnetic stirring bar was placed into the beaker and the beaker itself was kept on a magnetic stirring plate. The thick homogenized organic phase was then withdrawn into a syringe and injected through a needle into the PVA solution stirring at 400–500 rpm in the beaker. The emulsion thus formed was left stirring for 12 h to allow chloroform to evaporate away. After chloroform evaporation, the PLGA carrier suspension was retrieved and centrifuged at 600 rpm for 5 min. The centrifugation was repeated twice with distilled water to remove any remaining PVA.

For the fabrication of rigid geometric fibroin carriers (henceforth called fibroin carriers), the silk cocoons were cut into small pieces (<1 cm^2) and boiled with constant stirring in 0.02 M sodium bicarbonate (Na_2CO_3) solution at 100 °C for 90 min for the removal of sericin. The 'degummed' silk or fibroin, thus obtained, was rinsed three to four times with DI water to ensure total removal of sericin. Afterwards, the fibroin fibres were dried overnight at 60 °C in a drying oven and then dissolved in Ajisawa's reagent ($CaCl_2$:ethanol:water = 1:2:8 molar ratio) [41] at 80 °C for 90 min. The viscous solution thus obtained was dialyzed in DI-water until a conductivity of < 5 μS in the dialysing water was reached. The resulting fibroin solution was then centrifuged for 10 min at 10,000 rpm to remove undissolved fibroin and other particulate matter. Fibroin carrier designing through computer aided design (CAD) and fabrication by 3D inkjet printing was done according to method described in our previous works [42–44]. In brief, the fibroin biomaterial ink was prepared by adjusting the fibroin concentration to 40 mg/mL and adding PEG_{400} for better printability. Afterwards, a 'plus' (+) shape was designed in CAD and imported into the computer controlling an in-house built inkjet printer. The size of the carrier was kept at 2.5 mm in length and 0.5 mm in breadth for both the lines of the plus-like shape. For 3D printing, the deposition of each layer of fibroin ink was followed by the deposition of methanol on the exact same position for crosslinking the regenerated (liquid) fibroin or Silk I into the insoluble Silk II structure. The printed structures were removed after 100 layers of deposition. The carriers were then gently submerged in 70% ethanol for sterilization and air dried inside biological safety cabinet (BSC) before use in cell culture experiments.

2.3. Surface functionalization of PLGA and fibroin carriers

To improve adherence and subsequent spread of cells, the PLGA carrier surface was functionalized with vitronectin, which readily

adsorb on a variety of surfaces and also bind to cell membrane proteins called integrins. For this, 6.25 μg/mL of human recombinant vitronectin (PeproTech Ltd.) was dissolved in DI water and added to the PLGA carrier suspension which was then left overnight at 2–8 °C for allowing vitronectin to adsorb on their surface. For fibroin carrier surface functionalization, the printed fibroin carriers were carefully taken out of the ethanol, air-dried under sterile environment, and submerged in the cell adhesion molecule poly-L-lysine (PLL) (MW = 70–150k) diluted to 0.01% (w/v). The structures were then left overnight at 2–8 °C to allow the PLL coat their entire surface.

2.4. Culture of L929 mouse fibroblasts and PC12 rat neuronal cells

The L929 and PC12 cells were cultured at 37 °C and 5% CO_2 in medium-sized T75 culture flasks using DMEM-F12 (1:1) medium with high glucose and supplemented with 10% foetal calf serum (FCS), 1% penicillin-streptomycin, 1% glutamine, and 0.5% Amphotericin B (Fungizone™). On confluence, the cells were detached with 0.25% (w/v) trypsin–EDTA, extracted, centrifuged, and resuspended in serum free culture medium for use in 3D cell culture. For cell seeding, the cells were counted both with a haemocytometer slide and with an automated cell counter (Bio-Rad Laboratories, Inc.) with trypan blue.

2.5. Cell seeding on carriers

For L929 cells, the PLGA carriers were centrifuged and resuspended in culture medium, and serially diluted to 5 carriers/μL. Similarly, the cell suspension was serially diluted to 50 cells/μL. For allowing initial adherence of cells on carriers, 60-well Terasaki plates were used as they can be inverted to produce hanging drops where the cells can come in contact with carriers due to gravity. Each 20 μL well in the Terasaki plate was filled with 10 μL of PLGA carriers and 10 μL of cells, thus totalling to 50 carriers and 500 cells in each well. After 24 h, the carrier-cell suspension was transferred in replicates to V-bottom 96-well plates and more medium was added for cell proliferation. For PC12 cells, the fibroin carriers were removed from PLL solution and resuspended in culture medium. As fibroin carriers are too big and heavy for use with Terasaki well plates, they were directly seeded on V-bottom well plates whose conical shape also serve to bring cells and carriers in contact and avoid and cell adherence on well surface itself. One fibroin carrier and 1000 cells were seeded per well of a V-bottom 96-well plate and the remainder of the wells were filled with culture medium in one set of samples and with culture medium with added nerve growth factor (NGF) in the other sample set.

2.6. Characterisation and imaging of carriers and 3D carrier-cell constructs

PLGA carrier size distribution was analysed with a DLS Particle analyser (Malvern Mastersizer 2000). For light micrographs, the carrier-cell constructs were imaged with a Zeiss light microscope controlled by Zeiss Zen software. The morphology and size of the PLGA carriers and the 3D carrier-cell constructs were analysed with a scanning electron microscope (Hitachi S4800) at 1.5 kV voltage. For SEM sample preparation, the carrier-cell constructs were withdrawn from the Terasaki plate, collected in a 1.5 mL Eppendorf tube and centrifuged for 2 min at 600 rpm. The supernatant was discarded and 150 μL of PBS was added to the tube for washing away the remaining culture medium by centrifugation and discarding the supernatant PBS. The samples were then fixed by adding 150 μL of glutaraldehyde in the tube and leaving it for 5 h. Afterwards, glutaraldehyde was removed by centrifugation and the sample was completely dehydrated by adding 150 μL of hexamethyldisilazane and leaving for 2 h. The tubes were shaken gently and hexamethyldisilazane along with the suspended 3D constructs was taken out with a micropipette and gently poured on circular carbon tabs already stuck on the SEM stub. The sample on the carbon tabs was left to air dry overnight in a sterile fume cabinet and then taken for SEM imaging after it had completely dried.

Fibroin carriers with adherent cells were imaged after 24, 48 and 72 h of incubation under a wide-field fluorescence microscope (Nikon Eclipse LV100). Following incubation for the different time periods, the medium was carefully removed and the cell-carrier constructs in the well plates were gently washed with PBS. The sample was then fixed in 3.7% paraformaldehyde for 20 min, followed by washing with PBS and then added in 0.1% Triton X-100 for 10 min to enhance cell membrane permeability for fluorophores. Afterwards, the sample was washed with PBS and stained for 60 min with phalloidin-TRITC to label the cytoplasm and DAPI to label the nucleus. The labelled cells on carriers were washed twice with PBS to remove extra dyes and fresh PBS was added before imaging. Several micrographs were taken by focussing different parts of the 3D constructs lying at different focal planes in the Z axis, and stacked together to form a single Z-stacked image using a focus stacking software. The morphology and size of the fibroin carriers and the 3D carrier-cell constructs were analysed with a scanning electron microscope (FEI Inspect F) at 1.5 kV voltage. For SEM sample preparation, the cell-carrier constructs were fixed as described above for L929 cells, carefully retrieved from the well plates, placed on the carbon tabs and then air dried before imaging.

2.7. Live / dead cytotoxicity assay

Qualitative live / dead cytotoxicity was conducted to assess and rule out any potential toxicity from PLGA and fibroin to the cells. For the assay, 2500 L929 cells with 100 PLGA carriers per well, and cells without carriers as negative control, were added in replicates in a 96-well plate and incubated for 24 h at 37 °C and 5% CO_2. After 24 h, the culture medium was carefully removed and each well was washed with PBS. Meanwhile, calcein-AM and ethidium homodimer-1 (ETHD-1) were dissolved in PBS at the concentrations of 0.5 μL/mL and 1 μL/mL, respectively, to formulate the fluorophore-PBS solution. 50 μL of this fluorophore-PBS solution was added to the cells in each well and then incubated at 37 °C and 5% CO_2 for 15 min. All the wells were then washed with PBS and filled with fresh 150 μL of PBS. The cells were then imaged at 20x magnification with a fluorescence confocal microscope (Zeiss LSM 710), using three laser excitation wavelengths of 403, 488 and 543 nm. For the PC12 cells, the culture medium in the wells was removed and a serum-free medium containing 0.001% (v/v) SYTO 9™ (Invitrogen) and 0.0015% (v/v) propidium iodide (PI) were added into the wells. The well plates were then incubated for 30 min at 37 °C and 5% CO_2. Afterwards, the medium was removed and the wells were washed and filled up with PBS. The cell-carrier constructs in the wells were then imaged using a wide-field fluorescence microscope with a UV illumination source and appropriate filters for different fluorophores.

2.8. Cell metabolism / proliferation assay

The cell proliferation or metabolic activity rates were analysed for both 3D and 2D cultures at 24 h, 48 h and 72 h post-incubation using the fluorescence resazurin-resorufin (alamarBlue™) assay. For the assay, culture medium was carefully removed from the wells containing the cell-carrier constructs and 100 μM resazurin dissolved in PBS was added in the emptied wells along with assay-dependent (phenol-free and serum-free) culture medium to make a 10% resazurin concentration in the medium. In addition, three empty wells per plate were also filled with 10% resazurin solution in culture medium to obtain the background fluorescence intensities, which were later averaged and filtered out from the fluorescence intensity data of the cells. The well plates were then incubated for 4 h at 37 °C and 5% CO_2. After incubation, the reduced resorufin from the wells were carefully transferred well-to-well into black 96-well plates and the fluorescence intensity was measured with a fluorescence plate reader (FLx800, Biotek Instruments Inc.) at 540/635 nm.

2.9. Statistical analysis

Origin™ was used for all statistical analyses for comparing the cell proliferation or metabolic activity rates across different culture times and between 3D and 2D cultures and for plotting the resazurin-resorufin assay data. One-way ANOVA was used as the test of significance and the p-values of at least < 0.05 were taken as significant.

3. Results

3.1. Characterization of PLGA and fibroin carriers

The freshly fabricated carriers were characterized using light microscopy, scanning electron microscopy and dynamic light scattering (only PLGA carriers). Fig. 1 (a) show the light microscope images and 1 (c–d) show the scanning electron microscope images of the porous PLGA carriers along with their various sizes, surface morphology and pores. The porous structure allows free-flow of nutrient-waste and gas exchanges while also allowing for stronger adherence of the cells. Fig. 1 (b) show the light microscope images and 1 (e–f) show the scanning electron microscope images of fibroin carriers printed in a pre-designed shape (plus-like in this case) along with their surface morphology. The plus-like shape was adapted from our previous work on biological millimetre-scale self-propelled motors [44], and therefore, more geometric shapes can be fabricated and tested in future for 3D cell patterning research. The size distribution of the PLGA carriers was measured to be 10–150 μm in diameter with the peak range of 50–100 μm, as shown in the graph in Fig. 1 (g), using a dynamic light scattering (DLS) instrument.

3.2. Characterization of the carrier–cell constructs

Fig. 2 (a) shows the light micrograph of a hanging drop in a well of the inverted Terasaki plate containing L929 cells freshly incubated with PLGA carriers. The cells are drawn close to the carriers under the influence of gravity in the hanging drop. Fig. 2 (b) shows the light micrograph of a well of the upright Terasaki plate after 12 h of incubation where the cells have begun adhering to the carriers. The number of cells adhering on an individual PLGA carrier was variable depending on the size of the carrier. Fig. 2 (c) shows the light micrograph of a carrier-cell construct extracted after 24 h of incubation in Terasaki plate. Here, the L929 cells can be seen adhering very strongly to the PLGA carriers while also being able to maintain their native spherical shape. The PC12 cells seeded on and incubated with fibroin cell carriers were imaged at 24 h, 48 h and 72 h post seeding with the fluorophore phalloidin-TRITC (red). The fibroin cell carriers inadvertently showed absorption of the fluorophores resulting in significant background noise. Z-stacked wide-field composite images of carrier-cell constructs are shown in Fig. 2 (d–f). The cells showed prominent adherence and visually evident proliferation in number which was later confirmed with cell proliferation or metabolic activity assay. Culturing the PC12 cells in the medium added with nerve growth factor (NGF) showed stronger adherence, spreading of cells and onset of differentiation as shown in the fluorescence images in Fig. 2 (g–i), which was later confirmed with scanning electron microscopy. The fibroin carriers, thus, not only aid neurons maintain their natural morphology in 3D culture as observed in Fig. 2 (d–f), but also facilitate axon and dendrite growth for neuron patterning. Differently shaped carriers can thus be fabricated as needed for nerve guidance as observed in Fig. 2 (g–i).

Fig. 3(a–d) shows the scanning electron micrographs of the 3D carrier-cell constructs retrieved after 24 h of incubation of L929 cells with PLGA carriers. Cells are observed to be adhering strongly even after the rough procedure of sample preparation for scanning electron microscopy, during which a majority of the adhering cells fell off. Cells undergoing division are also seen very clearly with the cytokinesis constrictions indicated by red arrows. Fig. 3 (e–h) shows the scanning electron micrographs of NGF-doped PC12 cells on fibroin carriers where several cells clearly show the onset of differentiation initiated by NGF and marked by the distinctive growth of cytoplasmic extensions and dendrites. Some of the cells show cytoplasmic extensions indicated by red arrows while some others show dendritic growths indicated by blue arrows.

3.3. Live/dead assay

Fig. 4 (a–b) shows almost no cytotoxicity in the L929 cells grown in 96-well plates with PLGA carriers and assayed after 24 h of incubation. The cell-permeable and non-fluorescent calcein-acetoxymethyl (calcein-AM) gets cleaved metabolically only inside live cells releasing the green fluorescent calcein. On the contrary, the red fluorescent cell-impermeable ethidium homodimer-1 (ETHD-1) binds only to the nucleic acids of dead cells where the nucleic acids are exposed. Some cells are seen adhering to the PLGA carriers while most can be seen fallen off during to the sample dyeing procedure. The PLGA carriers also adsorbed the red colour of ETHD-1, however, their large size clearly distinguishes them from the much smaller dead cells, few of which can be observed in the images. Similarly, Fig. 4 (c–d) shows no evidence of cytotoxicity in the PC12 cells which were incubated with fibroin carriers in 96-well plates and assayed after 24 h with fluorophores SYTO 9 and propidium iodide. The cell-permeable SYTO 9 binds to the nucleic acids of live cells. On the contrary and similar to ETHD-1, the red fluorescent cell-impermeable propidium iodide (PI) binds only to the nucleic acids of dead cells where the nucleic acids are exposed. The fibroin cell carriers inadvertently showed mild adsorption of the fluorophores resulting in background fluorescence noise. The PC12 cells took up the membrane permeable SYTO 9 and showed its green fluorescence while the red fluorescence of impermeable PI was not observable, suggesting that very few to no cells became non-viable while adhering to the fibroin carriers. Similar to the L929 cells, the PC12 cells showed prominent adherence but sloughed off the carriers in significant quantities during the sample staining process.

3.4. Cell metabolic activity assay

During the resazurin-resorufin (alamarBlue™) assay, the blue-coloured, non-toxic, cell-permeable and non-fluorescent resazurin gets reduced to the pink-coloured and fluorescent resorufin through a reaction which occurs in the mitochondria and is catalysed by the enzyme NADPH dehydrogenase. Thus, the more the number of cells the more will be the resorufin content and the resulting fluorescence intensity. Fig. 5 shows significant increase in the fluorescence intensities of both L929 cells and PC12 cells in their respective 3D cultures after 72 h of incubation in comparison to the values after 24 h and 48 h. Additionally, in case of L929 cells, the wells containing cells incubated with PLGA carriers (3D culture) show much higher fluorescence than the wells having only cells (2D culture) after the same time intervals of 48 and 72 h. A plausible explanation for this observation could be that as the PLGA carriers provide a 3D platform and also increase the surface area for the cells to grow on, there would be more cells in the wells containing PLGA carriers, whereas, in the cell-only wells, the flat two dimensions of freedom and limited surface area would act as the limiting factor for cell proliferation. Nonetheless, in case of PC12 cells, no significant difference in the cell proliferation rates could be observed between the 3D (cells with fibroin carriers) and 2D (cells only) cultures. The plausible reason behind this could be the well-observed phenomenon of clustering or aggregation of neuronal cells, such as PC12 cells, *in vitro* when a high enough cell density is reached. Such cell clusters are one of the two morphologies, with the other being the regular separated cells, in which several neuronal cell lines tend to exist [45,46]. In such a situation, the clustered cells would tend to fall off the carriers under their mass and lose viability or undergo apoptosis if they become too big. Therefore, unlike L929 cells, there is an observed limitation in the

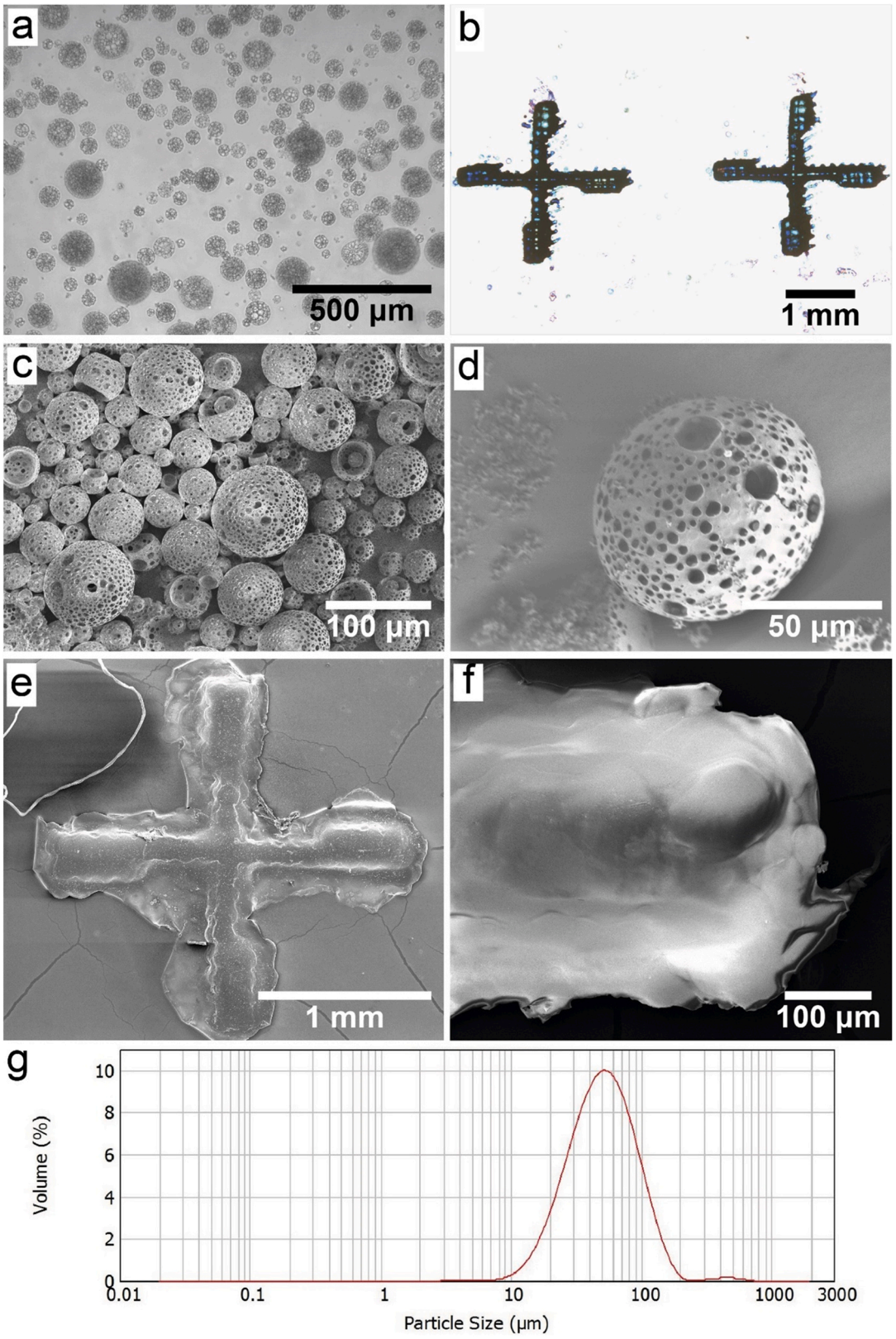

Fig. 1. (a, b) Light micrographs of (a) freshly fabricated spherical porous PLGA carriers showing its morphology and size diversity, and (b) freshly printed fibroin carriers in a required shape (plus-like in this case). (c, d) Scanning electron micrographs of PLGA carriers of various sizes at two magnification levels showing their topographical features, such as pores. (e, f) Scanning electron micrographs of 3D printed silk fibroin carriers at two magnification levels showing their topographical features, such as texture. (g) Dynamic light scattering data showing the size distribution of PLGA carriers in the graph generated by the DLS instrument. The peak carrier size range is approximately 50–100 µm.

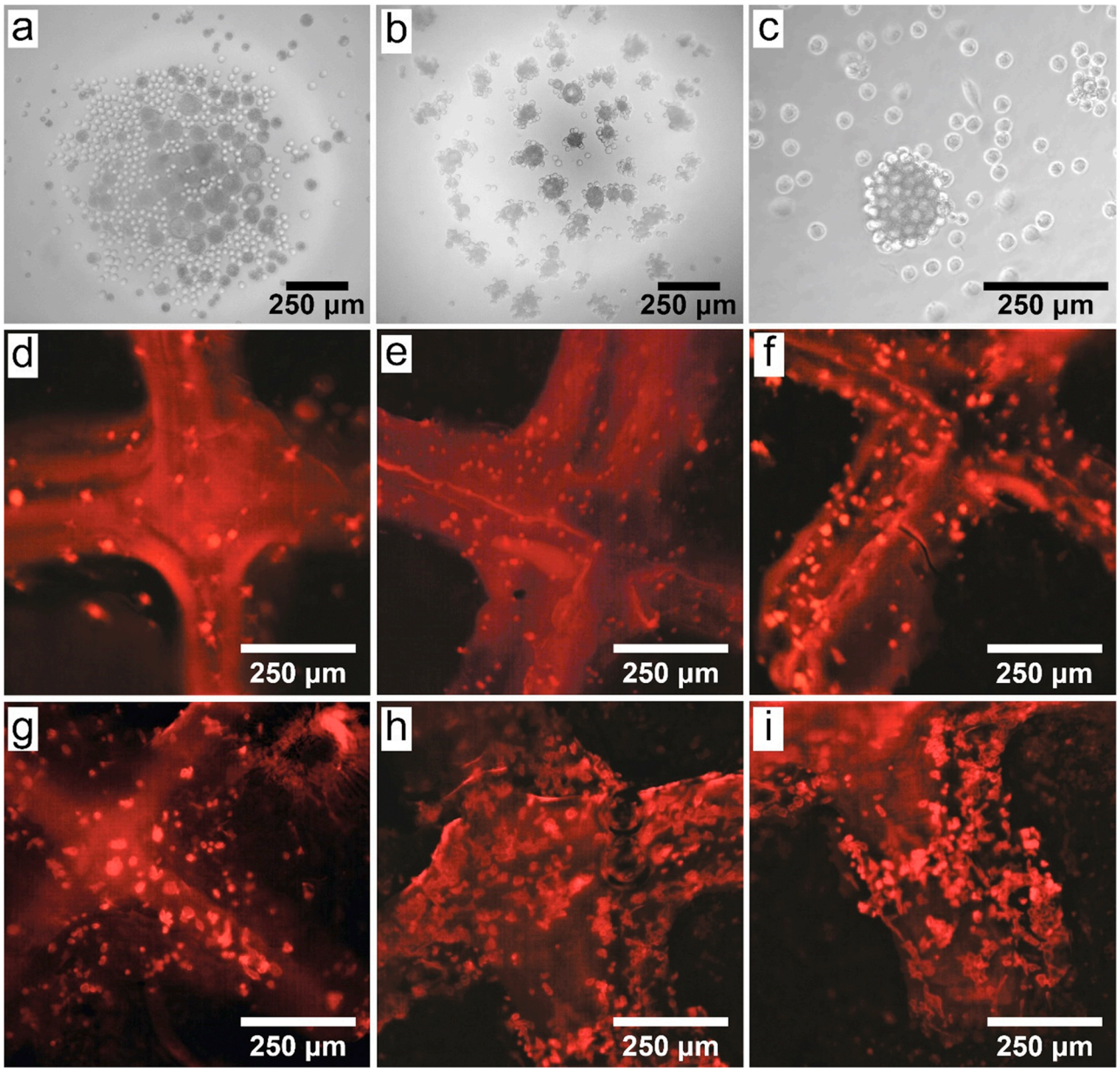

Fig. 2. (a) Light micrograph of a hanging drop in an inverted Terasaki plate containing L929 cells freshly incubated with PLGA carriers. (b) Light micrograph of L929 cells adhering on the surface of PLGA carriers in a well of an upright Terasaki plate after 12 h of incubation. (c) Light micrograph of a carrier-cell 3D construct extracted from a hanging drop of the Terasaki plate after 24 h of incubation showing strong adherence of the cells on the carrier (some sloughed off cells are also seen in the background). (d–f) Wide-field fluorescence z-stacked composite micrographs of PC12 cells adhering and proliferating on 3D fibroin carriers and imaged at (d) 24 h (e) 48 h (f) 72 h after incubation. The cells were stained with phalloidin-TRITC (red) which stains the cytoplasm. The fibroin itself absorbed a significant amount of fluorophore and caused background noise in fluorescence. The cells can be seen as small red spherical dots adhering and growing on the carriers. (g–i) PC12 cells cultured with nerve growth factor (NGF) show greater adherence, spread and growth of cytoplasmic extensions marking the onset of neurite growth as seen in the wide-field fluorescence z-stacked composite micrographs imaged at (g) 24 h (h) 48 h (i) 72 h after incubation.

proliferation of PC12 cells in the 3D culture environment.

4. Discussion

The main achievement of this study is the demonstration of an easy to fabricate, biocompatible, economical, and free-floating platform for the adherence, culture, proliferation and directed growth of mammalian cells while they are able to maintain their native spherical shape. Such physiologically relevant 3D culture platforms hold the potential to make the results and the interpretations of cell-based research more accurate and, thus, replace animal testing to a great extent in the fields of drug discovery, development of disease models, cancer and tumour research, cosmetics research and regenerative medicine research. As studied here, one important implication is the rapid *in vitro* cell proliferation without loss of function in cells and without the need for repeated passaging. This is helpful in such areas as adoptive cell transfer procedures, *e.g.*, stem cell therapy and cancer immunotherapy, which involve *ex vivo* gene editing, *in vitro* proliferation and transplantation of the genetically edited cells back into the patient. Another important implication is *in vitro* brain tissue and ganglion models for the understanding of neurodegenerative diseases and *in vitro* patterned neuronal culture for developing nerve tissue grafts for the treatment of neurodegenerative diseases. Different assessments, such as characterisation of 3D cell-carrier constructs, cytotoxicity assay and cell metabolic activity assay,

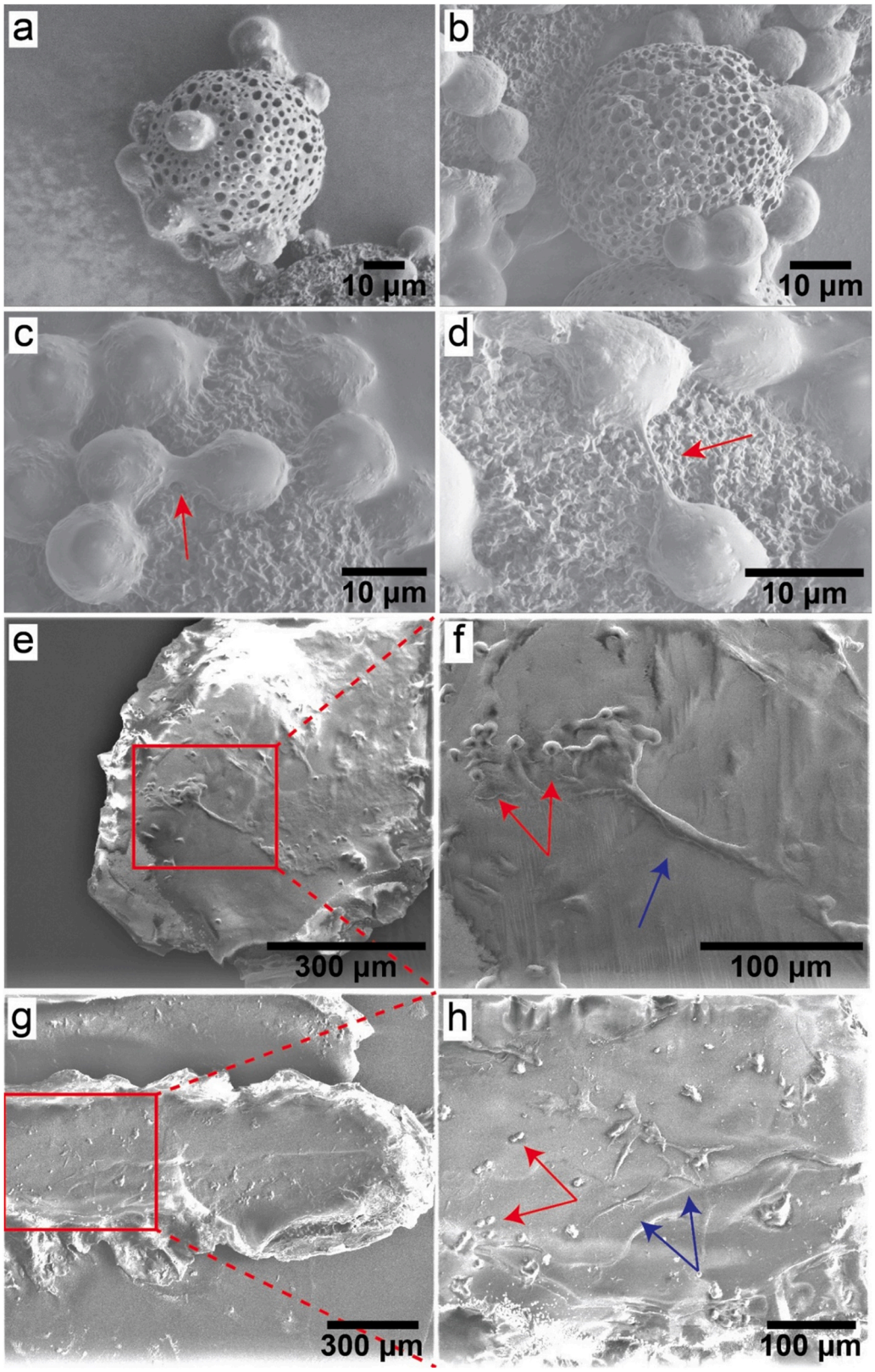

Fig. 3. (a–d) Scanning electron microscope (SEM) images of 3D culture of L929 fibroblasts on porous PLGA carriers showing strong cell adherence and division. The constrictions between the dividing cells undergoing cytokinesis are indicated by arrows in red colour. Several cells sloughed off the PLGA carriers during the SEM sample preparation procedure. (e–h) SEM images of the 3D culture of PC12 neuronal cells on fibroin carriers in medium containing nerve growth factor (NGF) and imaged after 7 days. The red arrows indicate undifferentiated cells, while the blue arrows indicate differentiating cells along with significant cytoplasmic extensions and neurite growth. The sample preparation for SEM caused a significant number of cells to slough off.

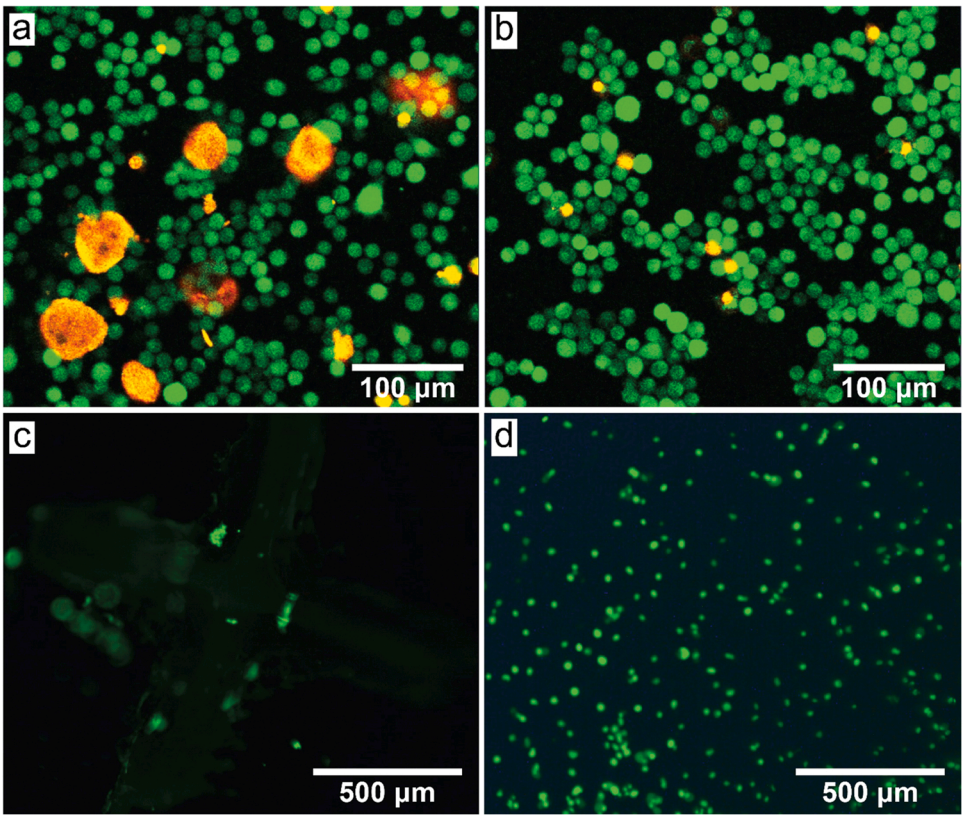

Fig. 4. (a, b) Fluorescence confocal micrograph showing L929 cells incubated, (a) with PLGA carriers and (b) without PLGA carriers, in a 96-well plate for 24 h. The live cells cleave the fluorophore calcein-AM to calcein which appears green on excitation. The small yellowish-red dots are dead cells whose exposed DNA take up the fluorophore ETHD-1. The PLGA carriers also inadvertently appear reddish due to ETHD-1 absorption. Several cells sloughed off the PLGA carriers during the fluorophore-staining procedure. (c, d) Fluorescence wide-field micrograph of PC12 cells incubated, (c) with fibroin carriers and (d) without fibroin carriers, in a 96-well plate for 24 h. The live cells took up the fluorophore SYTO 9 which appears green on excitation. No dead cells stained by propidium iodide were visible. Very few cells are observable on the carrier as the majority of the cells got washed away during the fluorophore-staining procedure. The fibroin also inadvertently absorbed the fluorophores causing mild background fluorescence noise.

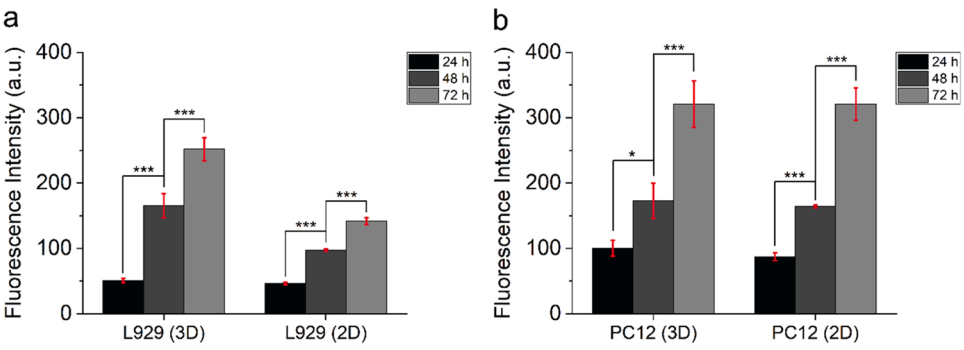

Fig. 5. Cell proliferation or metabolic activity as determined by measuring mean fluorescence intensity (F. I.) in arbitrary units (a. u.) from the resazurin-resorufin (alamarBlue™) assay. The fluorescence intensities were measured after 24 h, 48 h and 72 h of incubation. (a) L929 cells were incubated with PLGA carriers (3D culture) and without PLGA carriers (2D culture) in 96-well plates. Significant cell proliferation was observed after 48 h when compared to 24 h and after 72 h when compared to 48 h (significance taken at $p < 0.001$ and denoted by ***). Also, significantly larger cell proliferation was observed in 3D culture after 72 h in comparison to 2D culture after 72 h (significance taken at $p < 0.05$). (b) PC12 cells were incubated with fibroin carriers (3D culture) and without fibroin carriers (2D carriers) in 96-well plates. Significant cell proliferation was observed after 48 h when compared to 24 h and after 72 h when compared to 48 h (significance at $p < 0.001$ is denoted by *** and at $p < 0.05$ is denoted by *).

were conducted to ensure the suitability of a biocompatible and biodegradable synthetic polymer, such as PLGA, and natural polymer, such as silk fibroin, to act as three-dimensional carriers of adherent mammalian cells, such as L929 mouse fibroblasts and PC12 rat neuron-like cells. These assessments have returned favourable results and, therefore, facilitate the future development of more complex on-carrier 3D cell and tissue culture models. Fig. 6 (a) shows a light micrograph of L929 cells in the conventional 2D culture in a contrasting comparison to Fig. 6 (b) which shows the light micrograph of a carrier-cell construct extracted after 24 h of incubation in a Terasaki plate. Similarly, Fig. 6 (c) shows a fluorescence image of PC12 cells in the conventional 2D culture in a stark comparison to Fig. 6 **(d)** which shows the fluorescence image of a carrier-cell construct extracted after 48 h of incubation.

5. Conclusion and future prospects

In the present study, we have shown two different kinds of on-carrier 3D cell culture models aimed at two distinct objectives – one is 3D cell proliferation with the maintenance of native spherical cell shape and the other is 3D neuronal cell growth, spread and differentiation. While there is no difference between the X – Y axes of 2D and 3D cultures, the cells in 2D lose their 'thickness' in the Z axis under the influence of gravity. In comparison, 3D culture allows versatility in the cell shape and size in all the three dimensions. This impact of the physical environment on cell structure causes morphological and physiological differences between the cells cultured in 2D and 3D. Virtually any field of research that requires cell-based experiments benefits from 3D cell cultures owing to their superior and more accurate replication of *in vivo* physiology. This work has shown that porous PLGA carriers and inkjet printed fibroin carriers are good prototypes for easy-to-fabricate free-floating 3D cell-

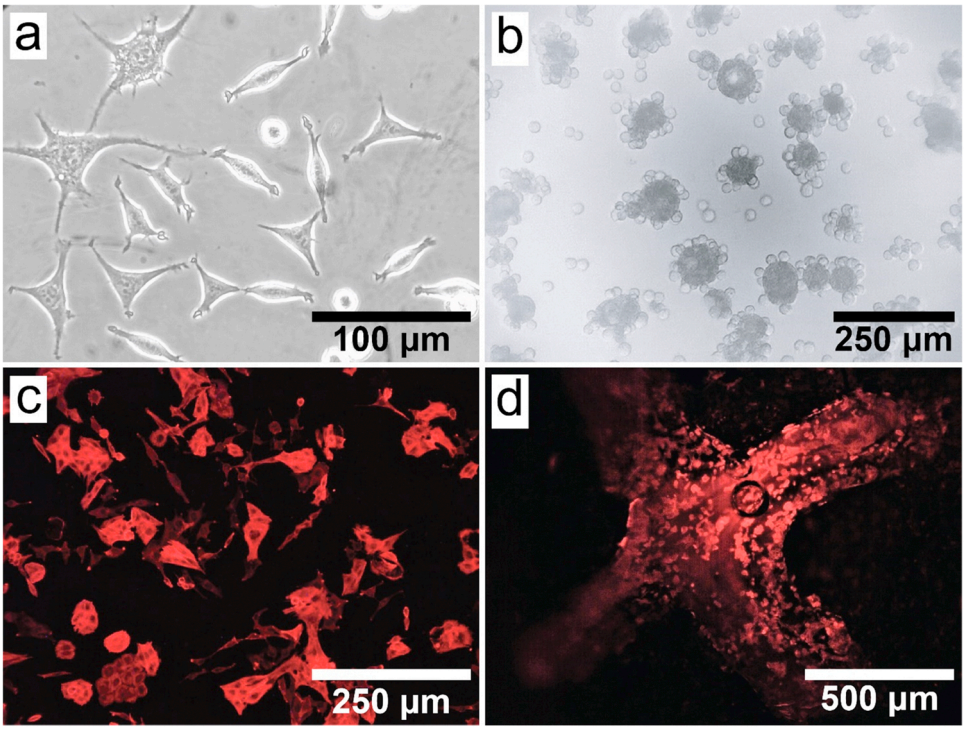

Fig. 6. Comparison between conventional 2D culture and 3D culture of cells on free-floating carriers with regard to different applications such as **(a, b)** maintenance of cell shape, polarity and proliferation and **(c, d)** cell shape, polarity and proliferation and, after the addition of nerve growth factor, spreading and patterned growth.

carriers. The results also represent the versatility, diversity and universality of the biocompatible, chemically stable, mechanically rigid and geometrically flexible 3D polymeric carriers for cell attachment, proliferation and spreading. Additionally, unlike 3D cell spheroids, in which necrosis of the core cells is a common occurrence, the approach in this study doesn't have a size or cell number limitation. As cells divide, more free-floating carriers can be added in the culture or bioreactor to accommodate the increasing cell population instead of continually passaging them. Furthermore, as the cells are inherently sensitive to their microenvironment in which they reside along with the 'niche' cells, more research with co-cultures will be required to standardise these techniques and make them clinically feasible.

CRediT authorship contribution statement

Piyush Kumar: Conceptualization, Methodology, Software, Validation, Formal analysis, Investigation, Data curation, Writing - Original Draft, Writing - Review & Editing, Visualization. **Ana Jimenez Franco:** Methodology, Validation, Formal Analysis, Investigation, Data Curation, Writing - Review & Editing. **Xiubo Zhao:** Conceptualization, Methodology, Validation, Resources, Writing - Review & Editing, Supervision, Project administration, Funding acquisition.

Declaration of Competing Interest

The authors declare that there is no conflict of interest.

Data availability

Data will be made available on request.

Acknowledgements

The authors would like to acknowledge the EPSRC (EP/N007174/1 and EP/N023579/1) for support. The authors would also like to thank Dr Zhidao Xia (Medical School, Swansea University, UK) for his intellectual input, guidance and supervision in the design and initial experimentations in this project.

References

[1] D.G. Harnden, Cell Biology and Cell Culture Methods—A Review, in: R.A. Harkness, F. Cockburn (Eds.), The Cultured Cell and Inherited Metabolic Disease: Monograph Based Upon Proceedings of the Fourteenth Symposium of The Society for the Study of Inborn Errors of Metabolism, Springer Netherlands, Dordrecht, 1977, pp. 3–15.
[2] J. Paul, Cell and tissue culture, Cell and tissue culture. (4th Edition) (1970).
[3] C.-P. Segeritz, L. Vallier, Chapter 9 - cell culture: growing cells as model systems in vitro, in: M. Jalali, F.Y.L. Saldanha, M. Jalali (Eds.), Basic Science Methods for Clinical Researchers, Academic Press, Boston, 2017, pp. 151–172.
[4] C. Jensen, Y. Teng, Is it time to start transitioning from 2D to 3D cell culture? Front. Mol. Biosci. 7 (2020) 33.
[5] H. Lodish, Darnell, J., Berk, A., Zipursky, L.S., Matsudaira, P., Baltimore, D., Integrating Cells into Tissues, Molecular Cell Biology, W. H. Freeman, New York, 2000.
[6] K. Von Der Mark, V. Gauss, H. Von Der Mark, P. MÜLler, Relationship between cell shape and type of collagen synthesised as chondrocytes lose their cartilage phenotype in culture, Nature 267 (5611) (1977) 531–532.
[7] O.W. Petersen, L. Rønnov-Jessen, A.R. Howlett, M.J. Bissell, Interaction with basement membrane serves to rapidly distinguish growth and differentiation pattern of normal and malignant human breast epithelial cells, Proc. Natl. Acad. Sci. USA 89 (19) (1992) 9064–9068.
[8] K. Duval, H. Grover, L.H. Han, Y. Mou, A.F. Pegoraro, J. Fredberg, Z. Chen, Modeling physiological events in 2D vs. 3D cell culture, Physiol. (Bethesda) 32 (4) (2017) 266–277.
[9] D. Dutta, I. Heo, H. Clevers, Disease modeling in stem cell-derived 3D organoid systems, Trends Mol. Med. 23 (5) (2017) 393–410.
[10] A. Birgersdotter, R. Sandberg, I. Ernberg, Gene expression perturbation in vitro—A growing case for three-dimensional (3D) culture systems, Semin. Cancer Biol. 15 (5) (2005) 405–412.
[11] C. Li, M. Kato, L. Shiue, J.E. Shively, M. Ares, R.-J. Lin, Cell type and culture condition–dependent alternative splicing in human breast cancer cells revealed by splicing-sensitive microarrays, Cancer Res. 66 (4) (2006) 1990.
[12] S. Ghosh, G.C. Spagnoli, I. Martin, S. Ploegert, P. Demougin, M. Heberer, A. Reschner, Three-dimensional culture of melanoma cells profoundly affects gene expression profile: A high density oligonucleotide array study, J. Cell. Physiol. 204 (2) (2005) 522–531.
[13] M. Delcommenne, C.H. Streuli, Control of integrin expression by extracellular-matrix, J. Biol. Chem. 270 (45) (1995) 26794–26801.

[14] E. Fuchs, T. Tumbar, G. Guasch, Socializing with the neighbors: Stem cells and their niche, Cell 116 (6) (2004) 769–778.
[15] M.J. Gomez-Lechon, R. Jover, T. Donato, X. Ponsoda, C. Rodriguez, K.G. Stenzel, R. Klocke, D. Paul, I. Guillen, R. Bort, J.V. Castell, Long-term expression of differentiated functions in hepatocytes cultured in three-dimensional collagen matrix, J. Cell. Physiol. 177 (4) (1998) 553–562.
[16] K.M. Yamada, E. Cukierman, Modeling tissue morphogenesis and cancer in 3D, Cell 130 (4) (2007) 601–610.
[17] E. Knight, S. Przyborski, Advances in 3D cell culture technologies enabling tissue-like structures to be created in vitro, J. Anat. 227 (6) (2015) 746–756.
[18] M. Hay, D.W. Thomas, J.L. Craighead, C. Economides, J. Rosenthal, Clinical development success rates for investigational drugs, Nat. Biotechnol. 32 (1) (2014) 40–51.
[19] R. Edmondson, J.J. Broglie, A.F. Adcock, L.J. Yang, Three-dimensional cell culture systems and their applications in drug discovery and cell-based biosensors, Assay. Drug Dev. Technol. 12 (4) (2014) 207–218.
[20] S. Kota, S. Hou, W. Guerrant, F. Madoux, S. Troutman, V. Fernandez-Vega, N. Alekseeva, N. Madala, L. Scampavia, J. Kissil, T.P. Spicer, A novel three-dimensional high-throughput screening approach identifies inducers of a mutant KRAS selective lethal phenotype, Oncogene 37 (32) (2018) 4372–4384.
[21] J.W. Haycock, 3D cell culture: a review of current approaches and techniques, in: J. W. Haycock (Ed.), 3D Cell Culture: Methods and Protocols, Humana Press, Totowa, NJ, 2011, pp. 1–15.
[22] A. De Pieri, Y. Rochev, D.I. Zeugolis, Scaffold-free cell-based tissue engineering therapies: advances, shortfalls and forecast, npj Regen. Med. 6 (1) (2021) 18.
[23] E. Carletti, A. Motta, C. Migliaresi, Scaffolds for Tissue Engineering and 3D Cell Culture, in: J.W. Haycock (Ed.), 3D Cell Culture: Methods and Protocols, Humana Press, Totowa, NJ, 2011, pp. 17–39.
[24] D. Baruffaldi, G. Palmara, C. Pirri, F. Frascella, 3D cell culture: recent development in materials with tunable stiffness, ACS Appl. Bio Mater. 4 (3) (2021) 2233–2250.
[25] S. Campuzano, A.E. Pelling, Scaffolds for 3D cell culture and cellular agriculture applications derived from non-animal sources, Front. Sustain. Food Syst. 3 (2019).
[26] S.A. Langhans, Three-dimensional in vitro cell culture models in drug discovery and drug repositioning, Front. Pharmacol. 9 (2018).
[27] S. Khetan, J.A. Burdick, Patterning network structure to spatially control cellular remodeling and stem cell fate within 3-dimensional hydrogels, Biomaterials 31 (32) (2010) 8228–8234.
[28] L. Naldini, Ex vivo gene transfer and correction for cell-based therapies, Nat. Rev. Genet 12 (5) (2011) 301–315.
[29] F.J.T. Staal, A. Aiuti, M. Cavazzana, Autologous stem-cell-based gene therapy for inherited disorders: state of the art and perspectives, Front. Pediatr. 7 (2019).
[30] G. Gowing, S. Svendsen, C.N. Svendsen, Chapter 4 - Ex vivo gene therapy for the treatment of neurological disorders, in: S.B. Dunnett, A. Björklund (Eds.), Progress in Brain Research, Elsevier, 2017, pp. 99–132.
[31] G. Consiglieri, M.E. Bernardo, N. Brunetti-Pierri, A. Aiuti, Ex vivo and in vivo gene therapy for mucopolysaccharidoses: state of the art, Hematol. Oncol. Clin. North Am. 36 (4) (2022) 865–878.
[32] S.T. Scanlon, Editing blood disorders, Science 371 (6524) (2021) 40.
[33] S. Bougioukli, R. Alluri, W. Pannell, O. Sugiyama, A. Vega, A. Tang, T. Skorka, S. H. Park, D. Oakes, J.R. Lieberman, Ex vivo gene therapy using human bone marrow cells overexpressing BMP-2: "Next-day" gene therapy versus standard "two-step" approach, Bone 128 (2019), 115032.
[34] K.U. Park, P. Jin, M. Sabatino, J. Feng, S. Civini, H. Khuu, M. Berg, R. Childs, D. Stroncek, Gene expression analysis of ex vivo expanded and freshly isolated nk cells from cancer patients, J. Immunother. 33 (9) (2010).
[35] M. Matsusaki, K. Sakaue, K. Kadowaki, M. Akashi, Three-dimensional human tissue chips fabricated by rapid and automatic inkjet cell printing, Adv. Healthc. Mater. 2 (4) (2013) 534–539.
[36] J. Loessberg-Zahl, J. Beumer, A. van den Berg, J.C.T. Eijkel, A.D. van der Meer, Patterning biological gels for 3D cell culture inside microfluidic devices by local surface modification through laminar flow patterning, Micromachines 11 (12) (2020) 1112.
[37] X. Yu, T. Zhang, Y. Li, 3D printing and bioprinting nerve conduits for neural tissue engineering, Polymers 12 (8) (2020) 1637.
[38] D. Joung, N.S. Lavoie, S.-Z. Guo, S.H. Park, A.M. Parr, M.C. McAlpine, 3D printed neural regeneration devices, Adv. Funct. Mater. 30 (1) (2020) 1906237.
[39] Q. Zhang, P.D. Nguyen, S. Shi, J.C. Burrell, D.K. Cullen, A.D. Le, 3D bio-printed scaffold-free nerve constructs with human gingiva-derived mesenchymal stem cells promote rat facial nerve regeneration, Sci. Rep. 8 (1) (2018) 6634.
[40] T.Z. Zhang, Q.Y. Zhang, J.S. Chen, K. Fang, J. Dou, N. Gu, The controllable preparation of porous PLGA microspheres by the oil/water emulsion method and its application in 3D culture of ovarian cancer cells, Colloid Surf. A 452 (2014) 115–124.
[41] A. Ajisawa, Dissolution of silk fibroin with calciumchloride/ethanol aqueous solution, J. Sericultural Sci. Jpn. 67 (2) (1998) 91–94.
[42] D.A. Gregory, P. Kumar, A. Jimenez-Franco, Y. Zhang, Y. Zhang, S.J. Ebbens, X. B. Zhao, Reactive inkjet printing and propulsion analysis of silk-based self-propelled micro-stirrers, Jove J. Vis. Exp. 146 (2019), e59030.
[43] P. Kumar, A. Legge, D.A. Gregory, A. Nichols, H. Jensen, S.J. Ebbens, X. Zhao, 3D printable self-propelling sensors for the assessment of water quality via surface tension, JCIS Open 5 (2022), 100044.
[44] P. Kumar, Y. Zhang, S.J. Ebbens, X. Zhao, 3D inkjet printed self-propelled motors for micro-stirring, J. Colloid Interface Sci. 623 (2022) 96–108.
[45] B. Wiatrak, A. Kubis-Kubiak, A. Piwowar, E. Barg, PC12 cell line: cell types, coating of culture vessels, differentiation and other culture conditions, Cells (2020).
[46] J. Kovalevich, D. Langford, Considerations for the use of SH-SY5Y neuroblastoma cells in neurobiology, in: S. Amini, M.K. White (Eds.), Neuronal Cell Culture: Methods and Protocols, Humana Press, Totowa, NJ, 2013, pp. 9–21.